CHARACTERIZATION OF HIGH-ENTROPY ALLOYS

Study of the addition of aluminum to the high entropy system HfMoTaTi+Al

Student: Daniel Costas Bosque
T7009T,Material Science & Engineering, project
Coordinators: Hanzhu Zhang & Farid Akhtar

2017 - 2018 Semester 1

CONTENT

ACKNOWLEDGMENTS

Firstly, I would like to express my very great appreciation to my coordinators Farid Akhtar and Hanzhu Zhang for the support during the whole process of this project: their patience and their guidance and their suggestions during the planning and development of this project. His willingness to give me their time whenever I had a question has been very appreciated.

I wish to acknowledge Roberts Joffe for his track of the project process and suggestions during the weekly meetings and the presentations.

I wish to acknowledge the help provided by Lars Frisk and Johnny Grahn for solving any question I had while using the equipment during the laboratory work.

I would also like to thank all the rest of members of the department, PhD and Master students with whom I shared such a wonderful time in Luleå.

Finally I would like to thank my family for their support and encouragement during my studies.

ABSTRACT

1. INTRODUCTION

High Entropy Alloys (HEA) are alloy systems that are formed with five or more principal elements of alloy or have an entropy of mixture higher than 1.5R. Although at first it may seem like if it is extrapolated from binary and ternary diagrams these supposed high entropy alloys may generate very complex microstructures with multiple phases, segregations and intermetallic compounds, making them very difficult to analyze and understand, however, due to the thermodynamics involved in a system with multiple components, HEAs tend to have simple crystal structure like body-centered cubic (BCC) and face-centered cubic (FCC).

Because of the first ideas that multiple elements alloys tend to have complicated microstructures and non-interesting properties, this field of study wasn't explored until the year 2004 when Jian-Wei Yeh and Brian Candor started investigating them. After the first studies, showing to the world that these new alloys presented interesting properties, publications related to High Entropy Alloys started increasing worldwide as it can be seen in Figure 1.

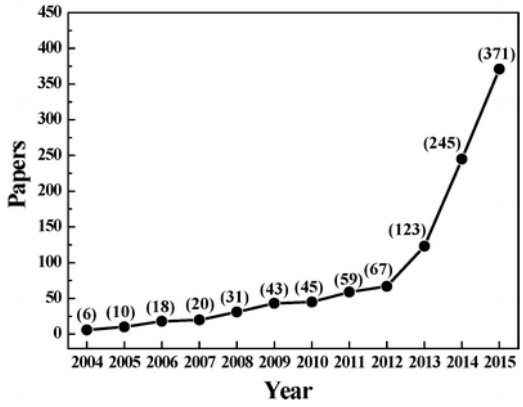

Figure 1: Number of articles published related to HEA systems. Obtained from [1].

As the investigation effort related to HEAs is increasing, the more it is becoming clear that HEA systems exhibit excellent characteristics such as high strength and hardness, excellent wear resistance, high-temperature strength, good structural stability, good corrosion and oxidation resistance over conventional alloys.

1.1. Scope of the project

The scope of this project is to study the effect of aluminum addition into the system HfMoTaTi. In order to achieve this goal the next experiments will be done:

- Ensure the stabilization of the BCC structure in the system HfMoTaTiAl.
- Check whether there is a reduction in the density of the system HfMoTaTiAl compared to HfMoTaTi.
- Characterize mechanical properties and hardness.
- Study the oxidation resistance of the system HfMoTaTiAl.

2. LITERATURE REVIEW

2.1. Definition of High Entropy Alloys

Conventional alloys have always been based in one or two principal elements, for example steel alloys are iron based, superalloys are nickel and cobalt based. High entropy alloys (HEAs) have two different possible definitions. The first definition that was attributed to them is that high entropy alloys are a new kind of metallic system that present at least five different principal elements, considering principal elements the ones that form at least 5 at% of the composition in the alloy [1]–[4]. The second definition that was used to describe them was related on the amount of mixing entropy that they were supposed to have. The other definition that has been used to mark the concept of high entropy alloys is the entropy of mixture. In this case it is considered that any alloy with a configurational entropy higher than 1.5R can be considered a high entropy alloy.

2.2. Thermodynamic fundamentals

It is known that when a system achieves its minimum Gibbs energy the system becomes stable.

If we take a look at the Gibbs energy equation:

$$G = H - TS$$

Equation 1: Gibbs energy equation

Where G is the Gibbs energy, H is the enthalpy, T is the temperature and S refers to entropy.

In case of HEAs how does enthalpy and entropy behave?

In the case of the mixing enthalpy of multiple elements, according to [5] it can be calculated from the regular solution model for n elements as it can be seen in Equation 2.

$$\Delta H_{mix} = \sum_{\substack{i=x \\ i \neq j}}^{n} \Omega_{ij} c_i c_j$$

Equation 2: Enthalpy mixture equation

In the case of the entropy in solid solutions entropy of an alloy with equimolar n-elements in an ideal solution state would be as it is specified in Equation 3:

$$\Delta S_{mix} = Rln(n)$$

Equation 3: Entropy mixture equation

Where *R* is the gas constant and *n* the number of elements.

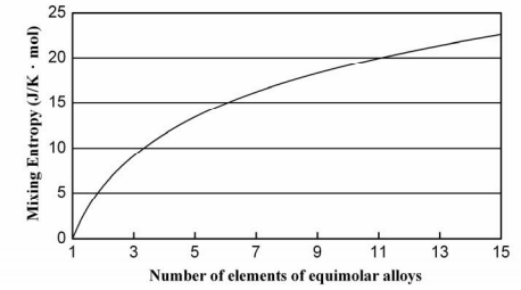

Figure 2: Entropy of mixing as a function of the number elements for equimolar alloys in completely disordered alloys.[4]

The minimum limit of five principal elements of alloys has been decided because it is considered the point in which entropy is high enough to generate a higher influence on the Gibbs energy compared to the mixing enthalpy effect. Therefore, high entropy solid solutions phases can be created. This is the main difference between ternary systems, in which the entropy is not high enough to overcome the effect of the enthalpy generating multiple phases including intermetallic compounds.

2.3. HEA's four core effects

According to [1], [2], [4], [6] there are four core effects of HEAs result to having multiple principal elements: High entropy, lattice distortion, sluggish diffusion and cocktail effects. High entropy is the effect that makes the material generate simplified solid solution phases, usually BCC and FCC. The sluggish diffusion effect helps reduce the kinetics in the microstructural level processes such as recrystallization, grain growth or creep. In the case of the lattice distortion it boosts mechanical and chemical properties. Finally in the case of the cocktail effect could be explained as a generation of composite effect properties in an atomic scale, improving the alloy's properties thanks to the interaction among the different elements compared the properties that would be expected using the rule of mixtures.

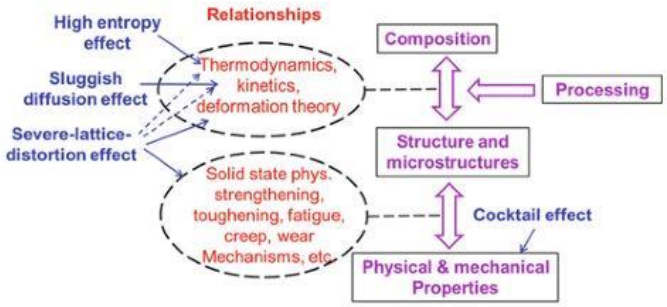

Figure 3: Scheme of core effects influence in physical metallurgy areas, obtained from [1]

2.3.1. High Entropy effect

High entropy effect is the main effect of this alloys. It allows the material to generate simple solid solutions structures such as BCC or FCC. These structures would be simpler than conventional alloys with two or three principal elements where there could appear multiple phases or even intermetallic compounds. In Figure 4 it can be seen how in quinary, senary and septenary have simple structures such as FCC and BCC.

To understand how high entropy boosts the generation of solution phases it is necessary to look at it from a thermodynamic point of view as it has been explained before: due to the high number of different elements in the mixture the mixing entropy increases up to the point that it reduces the Gibbs energy of simple structures such as FCC and BCC with all the elements in it. This reduction of the Gibbs energy stabilizes these high entropy phases creating a simple microstructure.

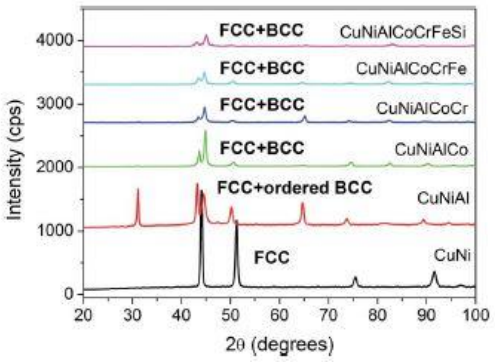

Figure 4: XRD patterns of a series of alloy designed by the sequential addition of an extra element to the previous one. All the alloys have one or two major phases that have simple structure, obtained from[2]

2.3.2. Sluggish diffusion effect

As it has been said, HEAs present multiple principal elements. As these elements generate a solid solution, it makes that each element is surrounded with its neighbors different one to another. In a diffusional process this takes importance due to the fact that when an element will have a different diffusion rate from one to another generating locations with high energy and lower energy.

During diffusion process if an atom has to move to a higher energy gap or a lower energy gap will make the diffusion process slower in both ways. In the case that it has to diffuse from a high energy point to a lower one the atom will be trapped to the lower energy point. In the opposite situation, if the atom has to diffuse from a low energy spot to a higher one, the atom will not only have to surpass a higher energy barrier but it also will tend to go back to its original location, making the diffusion process slower.

2.3.3. Severe lattice distortion

Due to the high-entropy effect HEAs tend to have a single matrix, either BCC, FCC or other structures. Consequently, all the elements are integrated to the same structure. As each element has its own different atomic size, different bonding energy with the other elements, and crystal structure tendency, the lattice of the resulting solid solution is severely distorted. In Figure 5 it can be seen a schematic of the lattice distortion.

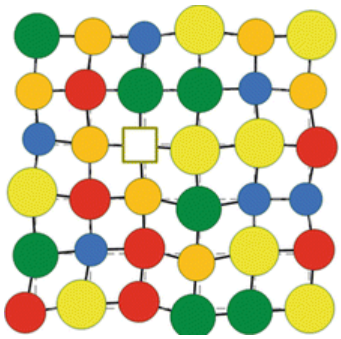

Figure 5: Schematic of a distorted lattice of a HEA [1]

As expected, lattice distortion affects the resultant properties of the resultant alloys such as hardness and strength due to the fact that lattice distortion hinders the movement of dislocations[2]. Another important effect is that it decreases the temperature dependence of these properties [4].

2.3.4. Cocktail effect

Because there are multiple principal elements in the alloy, HEAs can be considered as a composite in the atomic scale. This means that interaction between different elements provides properties higher than what the rule of mixtures would predict. Other impacts of the cocktail effect may also be the promotion of formation of a determined phase such as aluminum, which depending on its concentration it may generate BCC or FCC structures depending on its content, as well as increasing the hardness of the system as it can be seen in Figure 6.

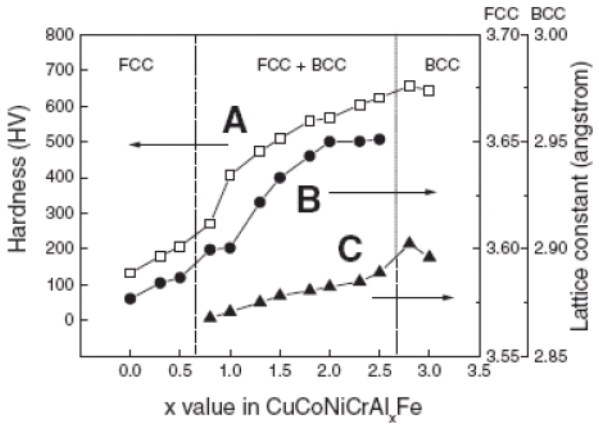

Figure 6: Strengthening effect of aluminum on cast hardened alloys AlxCoCrCuFeNi. A,B and C refer to hardness, FCC lattice constant and BCC lattice constant respectively [4].

2.4. HEA's microstructures

2.4.1. Solid Solubility according to Hume-Rothery rules

In order to achieve the creation of a HEA solid solution it is not only necessary to have multiple different elements but it is also important to make sure that these elements are compatible between them as not all elements can be mixed in one single system. Elements need to be similar in order be able to generate a solid solution. As a first approximation to understand what requirements should be expected for the case of HEAs it is good to take a look at the Hume-Rothery rules for binary substitutional solid solution:

1. The atomic radio of the solvent elements shouldn't be more than 15%.
2. The two elements must form the same crystal structures similar at least and preferably the same.
3. In order to achieve a complete solubility it is required to have the same valence.
4. Electronegativity should be similar in order to avoid the formation of intermetallic compounds.

In the case of HEAs the first Hume-Rothery rule can be upgraded considering how much is the similarity between all the atomic sizes of the elements of the alloy. In order to measure it is calculated according to the atomic size difference ratio (δ) as shown in

$$\delta = 100\sqrt{\sum_{i=1}^{n}\left(1-\frac{r_i}{\sum_{i=1}^{n}c_i r_i}\right)}$$

Equation 4: Method to calculate the atomic size difference ratio

Where r_i is the atomic radios and c_i is the atomic percentage of each element.

If the aspect ratio (δ) and the enthalpy of mixture are between the proper values, High Entropy Alloys can be generated as it can be seen in figure

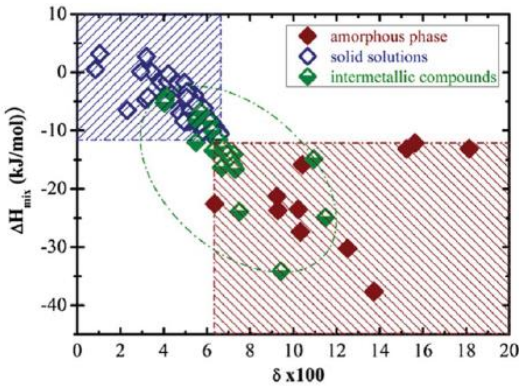

Figure 7: δ- H_{mix} plot delineating the phase selection in HEAs. Obtained from [1].

2.5. Mechanical properties of HEA's

2.5.1. Hardness

Hardness presents a wide variety inside the HEA family of materials. There are different factors that have to be taken into account in order to understand this wide range of values.

The first that can be taken into account is the fabrication process. Depending on whether the sample has been generated via liquid-state processing or solid-state processing the material will present different microstructure.

Another important point is the composition of the HEA system, depending on the elements that form the alloy, their properties and the bonds between them will determine the hardness of the alloy. For now the most studied high entropy alloys are the ones formed by the elements: Al-, Co-, Cr-, Cu-, Fe-, Ni-, Ti-, and V-based. In Figure 8 it can be seen the range of hardness for the systems made with the most studied elements.

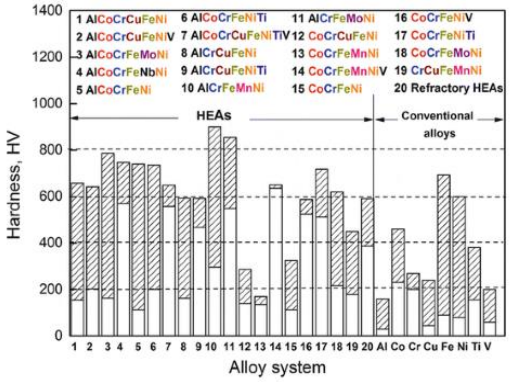

Figure 8: Maximum and minimum hardness of the most studied HEA systems.[1]

Another important factor determined by the components in the HEA is the possibility that they can modify the crystalline structure of the system. As there are crystalline structures like BCC harder than FCC[2], [6].

2.5.2. Compressive properties

As HEAs show superior mechanical properties under elevated temperatures, the compressive properties are commonly studied under both room temperature and high temperatures. According to J.W. Yeh [7], Al0.5CoCrCuFeNi high entropy alloy tends to have different behavior under different temperature and strain rates as it can be seen in Figure 9. If it is taken into a closer look there appear certain ups and downs in the plastic deformation regions at 873K, 973K, 1073K and 1173K. It implies the existence of multiple deformation mechanisms during compression test in high entropy system.

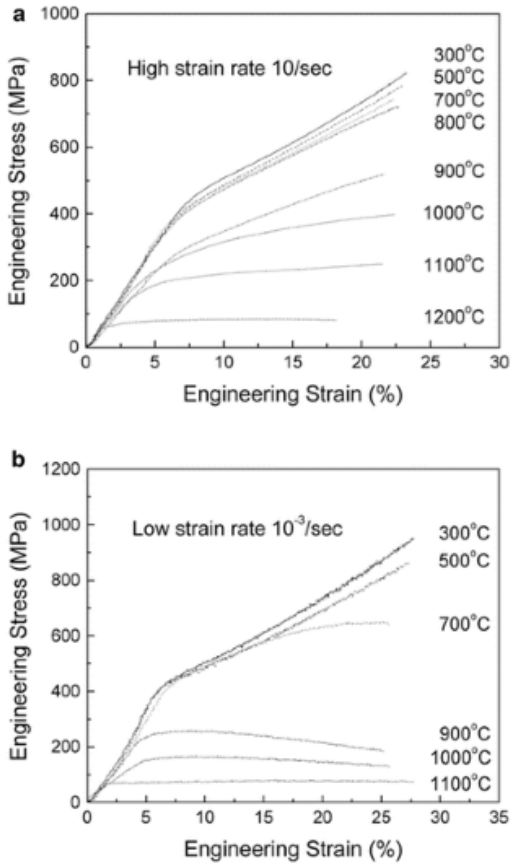

Figure 9: Compressive stress– strain curves of Al0.5CoCrCuFeNi at different temperatures and strain rates of (a) $10s^{-1}$ and (b) 10^{-3} s^{-1} [7]

2.6. Synthesis and Processing

2.6.1. Melting and casting

Melting and casting have become the most usual processes to fabricate HEAs, specially vacuum arc melting and vacuum induction melting processes. These technologies have been chosen especially due to the fact that they can reach temperatures high enough (around 3000°C) to melt metals that have high melting points. Although this seems like a good point on the side of this technologies, melting and casting processes generate as-cast microstructures. This means that dendritic microstructures subjected to segregation appear in the resultant samples. This can be seen in different articles such as [8]–[11].

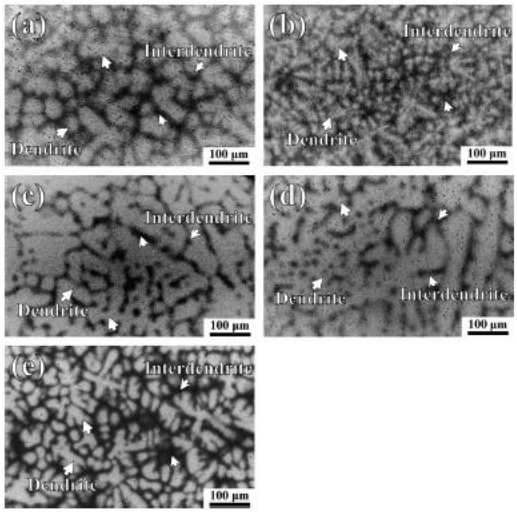

Figure 10: Backscattered electron images from HfNbTaTiZr, (b) Al0.3HfNbTaTiZr, (c) Al0.5HfNbTaTiZr, (d) Al0.75HfNbTaTiZr, and (e) AlHfNbTaTiZr obtained via vacuum arc melting.[9]

2.6.2. Solid-state processing

In the case of solid-state processing techniques, they have been less usual routes than the melting and casting processes.

In solid-state processes it is required a first mechanical alloying step. With this step a blend of the different elements that will form the HEA system will be made. Mechanical alloying is usually made via high-energy ball milling. This technique doesn't only disperses the powders into a mixture. It continuously breaks, deforms, fractures and welds them until the point that it modifies the composition of the powders generating solid-state alloy nanoparticles.

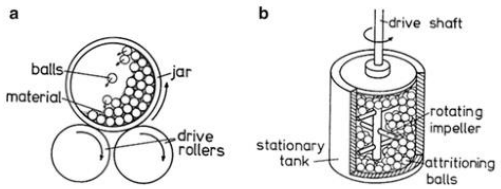

Figure 11: (a) Schematic cross-section of a tumbler ball mill. (b) Schematic of an attrition ball mill[1]

The advantages of this process is the versatility and the fact that it is done at room temperature. Because this process is made at room temperature it allows avoid possible segregation problems compared to what happens in liquid-state processing methods as it has been mentioned before. As in any case, this process also has its own disadvantages. The main disadvantage of this method is the possibility of contamination in the samples due to the milling media or atmosphere.

After the mechanical alloying process it is still required to sinter the samples. In order to achieve this goal the most common procedure is via Spark Pulse Sintering (SPS), also known as Pulse Current Processing (PCP).

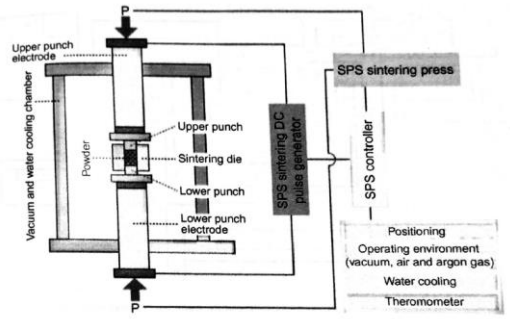

Figure 12: Schematic representation of operation of SPS.[6]

In this process the sample is covered in a layer of graphite in order to ensure a good conduction. The combination of high amperage pulse current, pressure and vacuum during PCP allow the sample to be sintered at relative low temperature and within a short time.

This process allows the generation of samples without dendritic microstructures, generating more homogeneous distribution of the elements in its microstructure.

2.7. Refractory HEAs

Refractory materials like Hf, Mo, Zr and V are materials that have high melting point (>1500^{o}C), which makes them desirable for high temperature applications.

Knowing the three first core effects that HEA provide makes them very interesting for high entropy alloys. If they are taken into account one by one, High-entropy effect helps achieve systems with a single phase, reducing the interphase energy. The sluggish diffusion effect would help reduce its creep in diffusion controlled creep situations. In the case of the lattice distortion, as it helps slow the creep effect in dislocation controlled creep situations.

In order to acquire refractory HEA systems the most used elements to create this compositions are elements that are used to create common refractory alloys.

2.7.1. Addition of aluminum in refractory HEAs systems

The effect of introducing aluminum in HEA systems has been studied [9], [12]. Among the different studies it has been demonstrated that the addition of Aluminum increases HEAs mechanical properties such as yield strength, Young's modulus and hardness although it reduces its fracture strain. Another important factor of incorporating aluminum to a HEA is the density reduction of the HEA in which it is incorporated.

One example of the study of the introduction of Aluminum in a HEA system is made by J.W. Yeh [9]. In this project it is studied how the introduction of aluminum affects the mechanical properties and the microstructure of the system $Al_xHfNbTaTiZr$. The samples contained an amount of Al of (x=0, x=0.3, x=0.5, x=0.75, x=1). In their study, the samples were fabricated via arc melting. Because it is a liquid-state process, the resultant microstructure had dendritic and interdendritic phase regions. These regions showed different concentrations of aluminum as it segregated in interdendritic region. In the cases of the sample (x = 1) this segregation made the creation of two different BCC crystal structures with different lattice parameters.

In the density of the samples it is demonstrated that the introduction of aluminum reduces the density of the alloy although it is not as much reduced as it would be expected from the rule of mixtures. It is thought that because aluminum has a stronger bonding with the rest of the principal elements.

Table 1: Theoretical density and experimental density of HEA systems studied in [8]

Alloy	Theor. density (ρ_{mix}, g/cm^3)		Exper. density (ρ, g/cm^3)
	Designed com.	Analyzed com.	
HfNbTaTiZr	9.89 ± 0.01	9.96 ± 0.01	9.72 ± 0.04
$Al_{0.3}$HfNbTaTiZr	9.39 ± 0.01	9.48 ± 0.01	9.53 ± 0.02
$Al_{0.5}$HfNbTaTiZr	9.25 ± 0.01	9.25 ± 0.01	9.34 ± 0.01
$Al_{0.75}$HfNbTaTiZr	9.02 ± 0.01	9.10 ± 0.01	9.27 ± 0.01
$Al_{1.0}$HfNbTaTiZr	8.56 ± 0.01	8.84 ± 0.01	8.91 ± 0.02

Stronger bonding of aluminum with the refractory elements also explain the reason why hardness increases more than it would be expected from the aluminum content of the samples. In the case of the compressive properties of the samples, the yield strength also increased with the amount of aluminum content, being coherent with the hardness results while the fracture strain decreased.

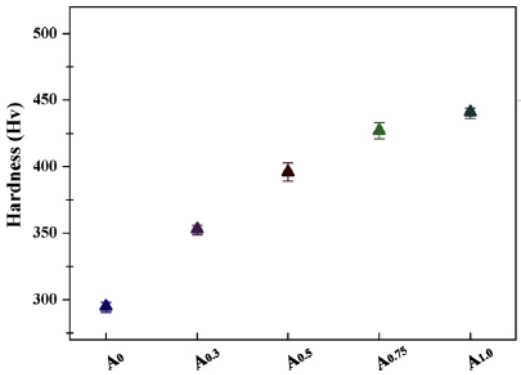

Figure 13: Hardness increment as the aluminum is introduced in systems studied in [8]

Another important point to take into account is that the fracture of the samples was through the interphase of the dendritic and interdendritic regions. This would mean that generating homogenous microstructure is expected to improve the compressive properties.

Another example of the study of the introduction of Aluminum in a HEA system is made by O.N. Senkov [12]. In this project it is studied how the substitution of a principal element for aluminum in the systems affect its properties. The original systems are $CrMo_{0.5}NbTa_{0.5}TiZr$ and HfNbTaTiZr. The modified systems with aluminum are $AlMo_{0.5}NbTa_{0.5}TiZr$ and $Al_{0.4}Hf_{0.6}NbTaTiZr$ respectively. Samples were produced via arc melting followed by Hot Isostatic Pressing (HIP) and annealing at 1673K and 207 MPa for 2 hours.

Microstructure was analyzed using SEM, microhardness and compressive behavior were also investigated. The compressive tests were done at several different temperatures: 298K, 873K, 1073K, 1273K and 1473K.

The substitution of chrome for aluminum in $CrMo_{0.5}NbTa_{0.5}TiZr$ system leads to the formation of single BCC phase without the brittle laves phase. It also helped decrease its density and increased the microhardness.

In the HfNbTaTiZr the partial substitution of Hf for aluminum retains the single BCC structure it already has, it reduces its density and increases its microhardness as can be seen in [12].

Table 2: Density of hardness of the alloys studied in [12] and its modified systems with the introduction of aluminum.

Alloy	ρ (g cm^{-3})	H_v (GPa)
$AlMo_{0.5}NbTa_{0.5}TiZr$	7.40 ± 0.08	5.8 ± 0.1
$Al_{0.4}Hf_{0.6}NbTaTiZr$	9.05 ± 0.05	4.9 ± 0.1
$CrMo_{0.5}NbTa_{0.5}TiZr$	8.23 ± 0.05	5.3 ± 0.1
HfNbTaTiZr	9.94 ± 0.05	3.8 ± 0.1

The yield strength evolution after adding the aluminum in the system is shown in Figure 14. It is important to see how the addition of aluminum increases the yield strength in all temperatures in $AlMo_{0.5}NbTa_{0.5}TiZr$. In $Al_{0.4}Hf_{0.6}NbTaTiZr$ system yield strength doubles at room temperature but as temperature increases the aluminum effect on the system becomes less relevant. This is attributed to the fact that the bonding between aluminum and the rest of the transition metals that at room temperature is very strong while it weakens as temperature increases, making it a less important factor as temperature rises.

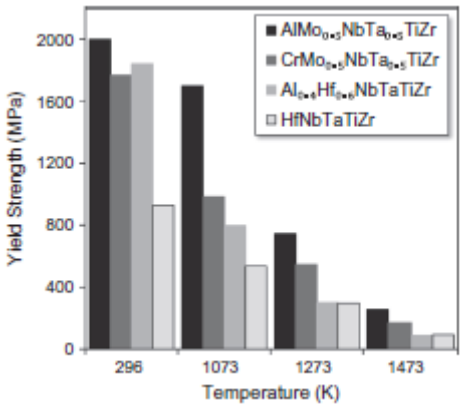

Figure 14: Yield strength of each system at the different studied temperatures.

About the microstructure of the samples of this study it has to be remembered that after the HIP process they were annealed, that is the reason why in this study HEAs don't have an as-cast dendritic microstructure. According to XRD results $AlMo_{0.5}NbTa_{0.5}TiZr$ presents two very similar BCC phases with different lattice parameter while $Al_{0.4}Hf_{0.6}NbTaTiZr$ presents one single BCC phase as can be seen in Figure 15.

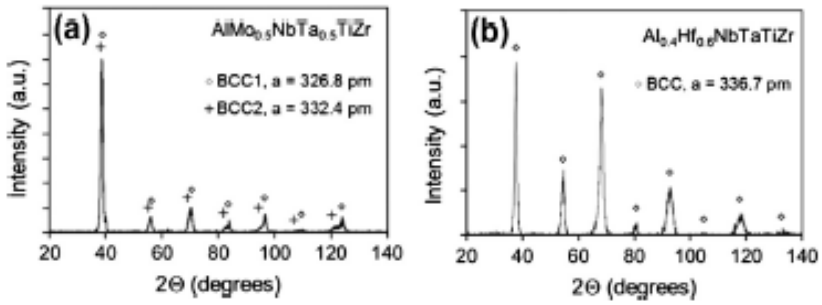

Figure 15: XRD results of the aluminum modified HEAs. Obtained from [12].

In the case of the $AlMo_{0.5}NbTa_{0.5}TiZr$ alloy it had a polycrystalline structure with a secondary phase in the grain boundaries of the polycrystalline matrix as well as nanoparticles of the same phase inside the grains of the main phase in a basked like lamellar structure.

According to Energy-dispersive X-ray spectroscopy (EDS) analysis, it has been identified that the second phase presents a higher concentration of aluminum while heavier elements: Mo, Nb and Ta have a higher concentration in the primary phase. Meanwhile the main phase the nanoparticles that can be seen in the lamellar structure have the same composition as the secondary phase.

2.8. Resume of the literature review

In this literature review, high entropy alloys were discussed. They are defined as alloys with five or more principal elements. It has also been studied how their core effects make high entropy alloys such an interesting research field. These core effects are: High entropy, lattice distortion, sluggish diffusion and cocktail effects. High entropy allows the alloy generate simple systems with one or two phases with simple crystalline structures. Lattice distortion increases the hardness of the phases due to large solution hardening effect. The sluggish diffusion due to the coexistence of multiple elements in the lattice hinders the diffusion process and makes transformations being able to generate supersaturated nanoparticles, diffusion barrier coatings, achieving high temperature strength and creep resistance. Finally the Cocktail effect helps improve HEAs properties even more than what would be expected from the rule of mixtures of the different elements of alloy thanks to the interactions between the different elements.

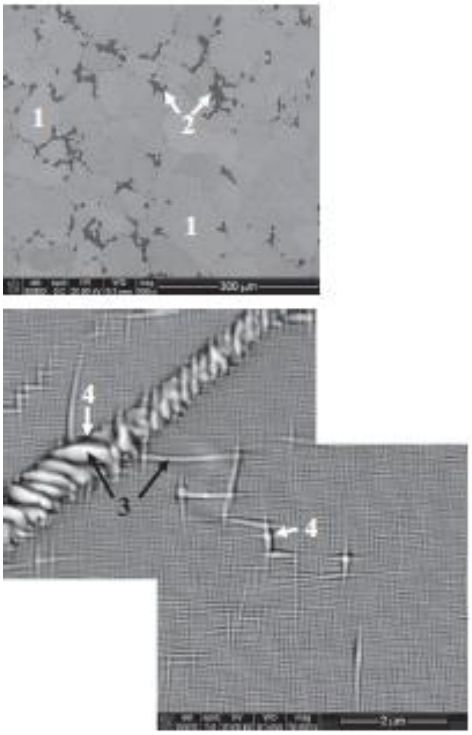

Figure 16: Backscattered image of the system $AlMo_{0.5}NbTa_{0.5}TiZr$. In the top image it can be seen the polycrystalline matrix and the secondary phase in the grain boundaries. In the bottom picture it can be seen the lamellar like structure inside the grains and the grain boundary. Obtained from [12].

There has also been studied the two main fabrication processes of HEAs. Melting and casting is the most used in research although it generates cast microstructures with important segregation between the dendritic and interdendritic phases, reducing the impacts of HEAs core effects. On the other side there is also the Solid-state processing that allows the generation of HEAs a more homogeneous microstructure although it requires a previous milling step of the powder previous to the spark plasma sintering process.

Finally the effect of incorporation of aluminum with refractory HEAs has been discussed. It has been determined that depending on the molar amount of aluminum added it may stabilize FCC, BCC or both structures. It has been determined that the addition of aluminum increases the hardness and the high temperature strength as well as decreasing the density of the HEA systems studied, making it a very interesting material for fields like aeronautics where light materials that have a good behavior at high temperatures are required.

3. THERMODYNAMIC AND GEOMETRICAL CALCULATIONS

In order to make sure that a high entropy disordered solid solution is acquired, first it is necessary that the mixture meets the thermodynamic and geometrical criterias. These parameters are: the mixing entropy, the mixing enthalpy and the difference in size between the different elements.

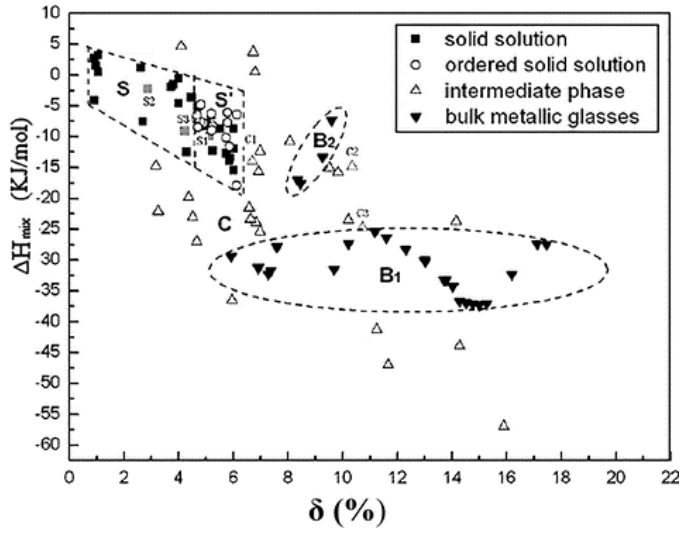

Figure 17: Phase selection diagram of HEAs and BMGs based on ΔH_{mix} and δ.

3.1. Mixing entropy

As the name of this family of compounds says, HEAs are required to have a high entropy. The entropy is supposed to be between 12J/Kmol and 17.5J/Kmol in order to form single phase solid solution. The high entropy is necessary to counterbalance the enthalpy in order to minimize the gibbs free energy of the system and therefore to stabilize it. The mixing entropy of the system is calculated as below: It can be seen that the mixing entropy S_{mix} meets the entropy criteria.

$$\Delta S_{mix} = k_B \ln w \quad (5.1)$$

$$\Delta S_{mix} = -R \sum_{i=1}^{n} X_i \ln X_i \quad (5.2)$$

$$\Delta S_{mix} = R \ln n = \mathrm{R} \ln 5 = 13.4 J/Kmol \quad (5.3)$$

Equation 5: HfMoTaTiAL system's ΔS_{mix} calculus.

$$\Delta G = \Delta H - T\Delta S$$

Equation 6: Free energy equation.

3.2. Mixing enthalpy

In order to be able to generate a solid solution not the mixing entropy is not the only parameter to take into account. The mixing enthalpy is another important parameter that not only competes against entropy in the free energy calculation but it also defines how much chemical interaction there is between the elements in the mixture in order to know how much atoms will tend to be surrounded of their same type of atoms o from other kind of atoms. In order to have the atoms as mixed as possible it is required to have a low enthalpy of mixture. The enthalpy of mixture should be between -20 kJ/mol and 5kJ/mol.

In order to calculate the enthalpy of mixture of the HEA system, values of the enthalpy of different binary systems were used. The data has been obtained from [13]. After making the calculus it could be confirmed that the high entropy alloy system HfMoTaTiAl has an enthalpy of mixture in between the recommended values.

$$\Delta H_{mix} = \sum_{i=1, i\neq j}^{n} 4\Delta H_{AB}^{mix}\, c_i c_j$$

Equation 7: ΔH_{mix} calculus method

Table 3: Enthalpy of mixture between the different elements present in the HfMoTaTiAl system

ΔH mix (kJ/mol)	Hf	Mo	Ta	Ti
Al	-39	-5	-19	-30
Hf		-4	3	0
Mo			-5	-4
Ta				1

$$\Delta H_{mix} = -16.32\ kJ/mol$$

Equation 8: HfMoTaTiAl's ΔHmix

3.3. Atomic size difference ratio

To generate the solid solution phase it is required to have a similar atomic size in order to avoid that the atoms are so different that they generate two different phases in order to release this strain. According to [1] the criteria for having

$$\delta(\%) = 100 \cdot \sqrt{\sum_{i=1}^{n} c_i \left(1 - \frac{r_i}{\bar{r}}\right)^2} \quad (9.1)$$

$$\bar{r} = \sum_{i=1}^{n} c_i r_i \quad (9.2)$$

Equation 9: δ calculus method.

Table 4: Atomic radius of the different elements present in the HfMoTaTiAl system

element	Hf	Mo	Ti	Ta	Al
atomic radius (pm)	150	154	136	138	118

$$\delta(\%) = 9.1$$

Equation 10: HfMoTaTiAl's δ result.

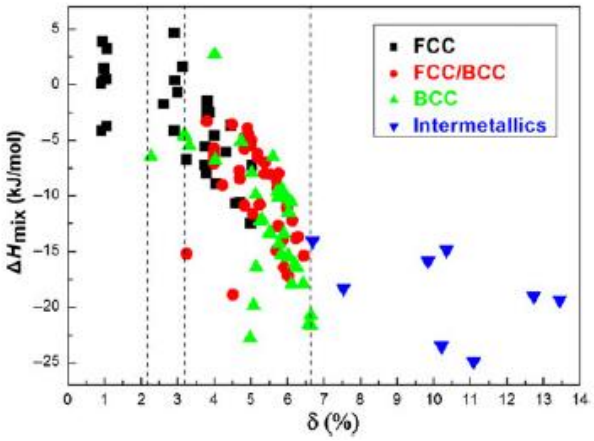

Figure 18: Dependence of crystal structures on the enthalpy of mixing, ΔH mix, and the atomic size mismatch, δ, in various HEAs[1]**.**

3.4. Omega

Another way to calculate the possibility to form a solid solution is with the parameter Ω. This parameter shows the relation between the minuend, the enthalpy of mixture, and the subtrahend, the temperature and the mixing entropy, as it can be seen on Equation 11. As it can be seen, the relation is direct. If $\Omega > 1.1$ it can be expected that that the HEA system will be stable as its free energy will be more influenced by the entropy factor instead of the mixture enthalpy.

$$\Omega = \frac{T_M \Delta S_{mix}}{|\Delta H_{mix}|} \quad (11.1)$$

$$T_M = \sum_{i=1}^{n} x_i (T_M)_i \quad (11.2)$$

Equation 11: Omega equation.

Where x_i is the atomic percentage of each alloy element and T_M is its melting temperature.

4. RAW MATERIALS AND SAMPLE PREPARATION

4.1. Starting materials used

In order to obtain the High Entropy sample the precursors used are elemental powders of the metals in that form the studied system. In Table 5 are described the particle size of each powder. In Table 6 it can be seen the crystal structure and lattice parameters of the different elements at room temperature.

Table 5: Particle size of the precursor powders used to sinter the samples.

Element	Particle size (μm) / mesh
Hf	1-3 /-
Mo	2-4/-
Ta	Max: 75 / 200
Ti	Max: 44 / 325
Al	Max: 44 / 325

Table 6: Crystal structure and lattice parameters of the different elements that compose the studied system.

Element	Crystal structure	a(Å)	c(Å)
Hf	Hexagonal	3.19	5.05
Mo	BCC	3.14	-
Ta	BCC	3.30	-
Ti	Hexagonal	2.95	4.69
Al	FCC	2.87	-
Average (Vergard's Law)	-	3.09	-

4.2. Mixing powders

All the starting powders were mixed by ball milling for 2 hours in order to have a homogenized powder before processing it. Stainless steel balls with a diameter of 4mm were used. The ball to powder ratio was 5:1.

4.3. PCP process

The alloy was fabricated by the solid-state technique Pulse Current Process because it is conducted under relatively lower temperature and within a shorter sintering time than the liquid-state process of arc-melting. It is expected to generate less segregation during the processing of the samples and it is a method closer to industry like application.

In order to design the processing route, the phase diagram of the studied system, HfMoTaTiAl was simulated with the software Thermo-calc. The simulation in Thermo-calc is conducted by deriving the thermodynamic properties and therefore minimizing the Gibbs energy in the system. Figure 19 shows the result of this simulation. From the CALPHAD simulation the window of the process parameters can be adjusted. In the studied case it can be seen that the minimum temperature from which the high entropy BCC structure can be formed is 800°C. The maximum temperature of the process is delimited by the melting temperature of the alloy. In this case the melting temperature is 1500°C.

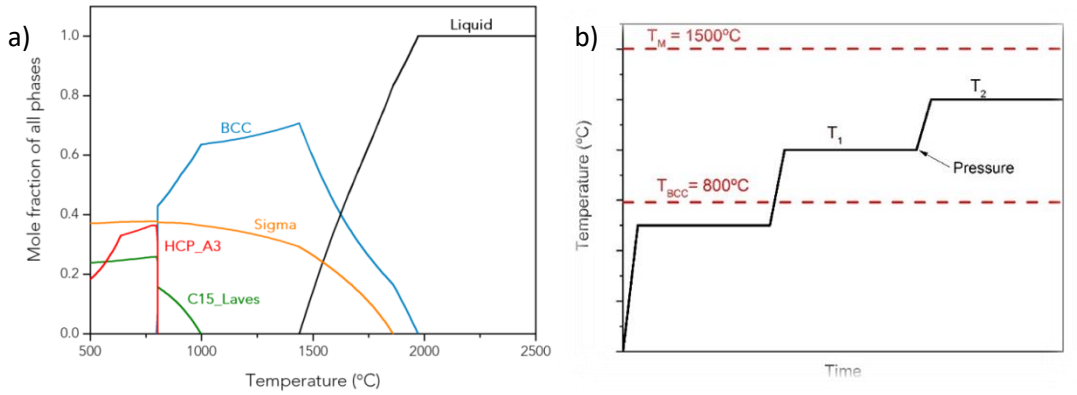

Figure 19. Simulated phase diagram of the system HfMoTaTiAl by the software Thermo-calc (a) and the designed sintering route (b):

Once the temperature range has been delimited the next step is decide how the temperature curve of the process will be. A three step sinter process was designed. The first step is always under the minimum temperature of the formation of the BCC structure. It is used to avoid that the aluminum powder melts before the formation of the BCC. T1 is the temperature at which the formation of BCC will start. After the T1 step a pressure will be implemented in the process and the temperature will be increased up to T2. This last step sinters the sample reducing its porosity. In order to determine the ideal temperature for each step, five different PCP route were performed. Table 7 shows the different temperature steps for each PCP process.

Table 7: Steps temperature during the PCP process for each sample

Sample	T_1(°C)	T_2(°C)
SPS 1	800	1000
SPS 2	850	1200
SPS 3	900	1350
SPS 4	1000	1250
SPS 5	1000	1250

Parameter Ω, explained in 3.4, was used to check whether the HEA system will be formed if instead of TM T2 is used in its calculus according to Equation 11: Omega equation. As it can be seen in Table 8 Ω >1.1 in all of the different temperature curves except of SPS 1 that is 1.0.

Table 8: Omega parameter calculated for each temperature curve.

Sample	Ω
SPS 1	1.0
SPS 2	1.2
SPS 3	1.3
SPS 4	1.2
SPS 5	1.2

5. EXPERIMENTAL PROCEDURES

In order to achieve the goals of the project, the experiments procedure was designed as follow: X-Ray Diffraction (XRD) of the samples in order to ensure BCC structure has been stabilized, Scanning Electron Microscope (SEM) and Energy Dispersive Spectroscopy (EDS) to confirm that the elements have been uniformly dispersed in the lattice. A density test in order to ensure that there has been a reduction of the density compared from the HfMoTaTi system. A hardness test has also been done to characterize the influence of aluminum in the alloy's hardness. Finally an oxidation resistance test was designed in order to analyze its resistance to high temperature conditions.

5.1. XRD

Samples were prepared to be analyzed polishing them until reach a mirror like surface. The equipment used to do the analysis is Panalytical Series 2 diffractometer with a copper anode K_α radiation, from 5° to 120°. XRD patterns were recorded at room temperature conditions.

5.2. SEM and EDS

SEM and EDS were made using a Scanning electron microscopy JSM- IT300 (JEOL, Tokyo, Japan). All samples were polished by following the metallographic procedure before the analysis. In at least 10 spot EDS were done in each sample in order to obtain a deviation of the lattice high entropy phase atomic composition.

5.3. Density

Density of the samples has been calculated using Archimedes water immersion method with a hydrostatic balance. Each sample has been measured three times in order to ensure the result doesn't show a high deviation.

5.4. Hardness

Hardness tests were done with Matsuzawa MXT-CX microhardness tester (Matsuzawa Co., Japan) at a load of 100N. Hardness measurements were made by measuring the diagonals of the indentation. Ten tests were done in each sample in order to obtain the results.

5.5. Oxidation resistance

Oxidation resistance tests were made with the sample SPS 3. The equipment used to do this experiment was NETZSCH TG-DTA/DSC STA 449 F3 Jupiter® (NETZSCH, Germany). The oxidation test conditions are shown in Table 9. The heating rate was 5K/min during the test and its weight have been recorded in order to understand the oxidation kinetics and oxidation resistance of HfMoTaTiAl HEA. The dimensions of the samples used in each test is shown in Table 10.

Table 9: Temperature and time of each oxidation resistance test.

Test	Temperature (°C)	Time (h)
1	1200	24
2	900	50

Table 10: Dimensions of the samples in each oxidation test.

Test	Length (mm)	Width (mm)	Thickness (mm)
1	3.96	1.97	1.82
2	3.45	2.75	1.85

5.5.1. Characterization of the oxide layer

After the oxidation test, the resultant oxide layer was characterized using SEM to study its morphology, EDS to analyze its chemical composition, XRD to study the phases present in it. A Micrometrics Gemini V 2390 apparatus (Micromeritics, Norcross GA, USA) was used to measure the porosity of the oxide layer after degassing the sample at 300 °C for 8 h.

6. RESULTS AND DISCUSSION

6.1. XRD

All five samples show similar XRD results as can be seen in Figure 21a. After indexing the peaks it could be confirmed that all the samples formed a BCC structure. The lattice parameters of the BCC structure are shown in Table 11. It could also be seen how the lattice parameters were very similar to the ones of the precursor elements with BCC structure (molybdenum and hafnium). Compare to the lattice parameters of the starting materials, Table 6 it can be seen that the samples lattice parameters are slightly higher than that calculated by the rule of mixture (the Vergard's law). The deviations from the Vergard's law in metal alloys are still unclear [1] but in the case of high entropy alloys there are two added factors that would modify the resultant lattice dimensions: The lattice distortion and the mixture enthalpy.

In the case of high entropy alloys, as it has been explained in previous pages of this work lattice distortion is one of its derived core effects. The fact that these alloys are composed by multiple components with different atomic sizes leads to a distortion of the lattice. This strain at which is submitted the lattice makes the atoms stay in a position that would not be the "equilibrium position" in non-distorted crystal. This offset of the atoms would increase the distance between them on average, increasing the lattice parameter as it is shown in Figure 20.

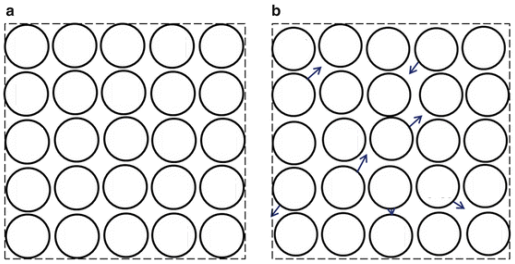

Figure 20: a. Equilibrium structure of a monoelement crystal b. Expanded structure of a monoelement crystal due to atoms being in an offset position.

The second factor that also effects the lattice stretching is the chemical bonds between the different elements. Having a negative enthalpy (like in the case of this sample) would reduce the bond length and therefore the lattice constant [1]. Therefore the lattice parameter of the studied alloy has a main factor stretching it and another factor reducing it.

Even though there is a confirmed high entropy phase in the samples there also appear some peaks that do not belong to this phase, marked with red asterisks on top of them in Figure 21b. After analyzing them it could be concluded that they do not belong to a cubic or hexagonal phase. Due to the limited diffraction intensity, the secondary phase was further investigated by SEM and EDS. Later on it could be concluded that it was a monoclinic hafnium oxide (HfO_2) phase. The peaks with a blue asterisk have been identified as a contamination in the Copper tube of XRD equipment and therefore they don't belong to the samples.

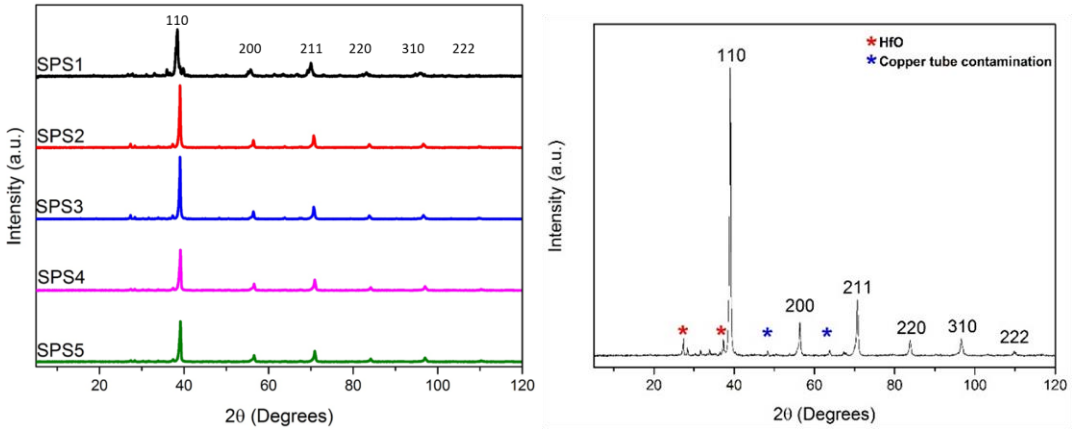

Figure 21a and 21b. 21a: XRD results of the samples 19b: Planes indexation of XRD results of SPS 4

Table 11: Lattice parameter of the samples

Sample	a(Å)
SPS 1	3.24±0.1
SPS 2	3.26±0.01
SPS 3	3.2±0.1
SPS 4	3.253±0.002
SPS 5	3.3±0.6

6.2. SEM and EDS

SPS1 showed the presence of Boron Carbide in its EDS results. It is due to a contamination during the mixture of the precursor elements. Therefore its results from SEM and EDS were discarded.

The microstructure of SPS4 and SPS5 in Figure 25 and Figure 26 shows uniform distribution of the different elements in the high entropy phase.

As it can be seen in the SEM results in Figure 23 and Figure 24, samples SPS2 to SPS 3 have areas with high concentration of tantalum and molybdenum. The average size of these tantalum and molybdenum rich areas is approximately 10µm. Comparing the size of these areas to the grain particles of the precursor powders in Table 5, it can be seen that molybdenum has a smaller grain size than the areas with high concentration of molybdenum. The reason of this may be that there still are agglomerated particles after milling process.

Another important point is that the higher concentration areas are that molybdenum and tantalum are the elements with higher melting temperature as shown in Table 12. As it is shown in Figure 22, the activation energy of self-diffusion is related to their melting temperature. This means that molybdenum and tantalum don't have enough energy to be able to diffuse in the HEA phase in low temperature curves like SPS 1 to SPS 3 while they have been able to diffuse in higher temperature conditions like SPS 4 and SPS 5.

The EDS results of all the samples (Figure 23 to Figure 26) also confirm the existence of a secondary phase that was expected from the XRD results. The chemical composition was determined using EDS mapping analysis of the surface. The secondary phase contains hafnium and oxygen which refers to hafnium oxide. In order check the origin of the oxide XRD was

performed on the powder of the hafnium precursor and it was concluded that it had hafnium oxide on it. Therefore the appearance of the hafnium oxide was not because of the process but because of the raw materials.

Table 12: Melting temperatures of the different elements that are part of the studied system.

element	Hf	Mo	Ti	Ta	Al
T_M (K)	2423	2890	1933	3269	933

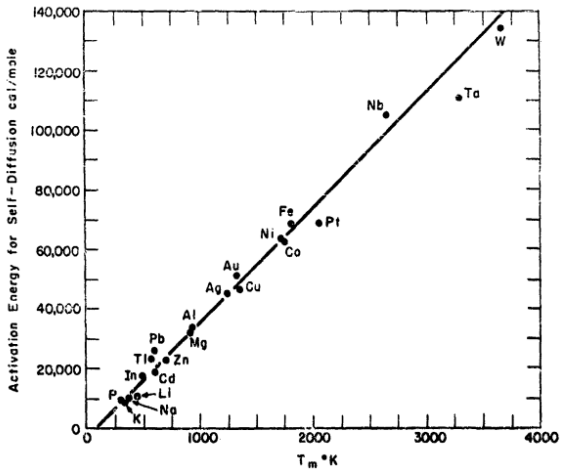

Figure 22: Relation between melting temperature and activation energy for self-diffusion in metals. Obtained from [14].

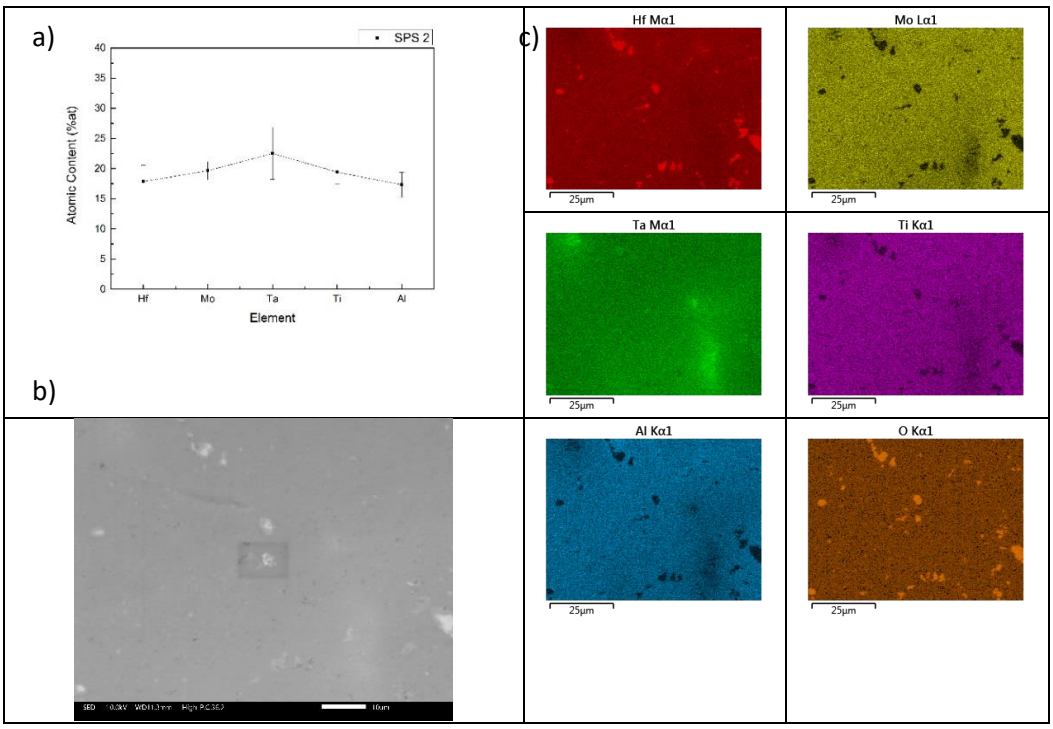

Figure 23: SEM and EDS results for SPS 2: Elements distribution(a), micrography(b) and mapping of sample(c).

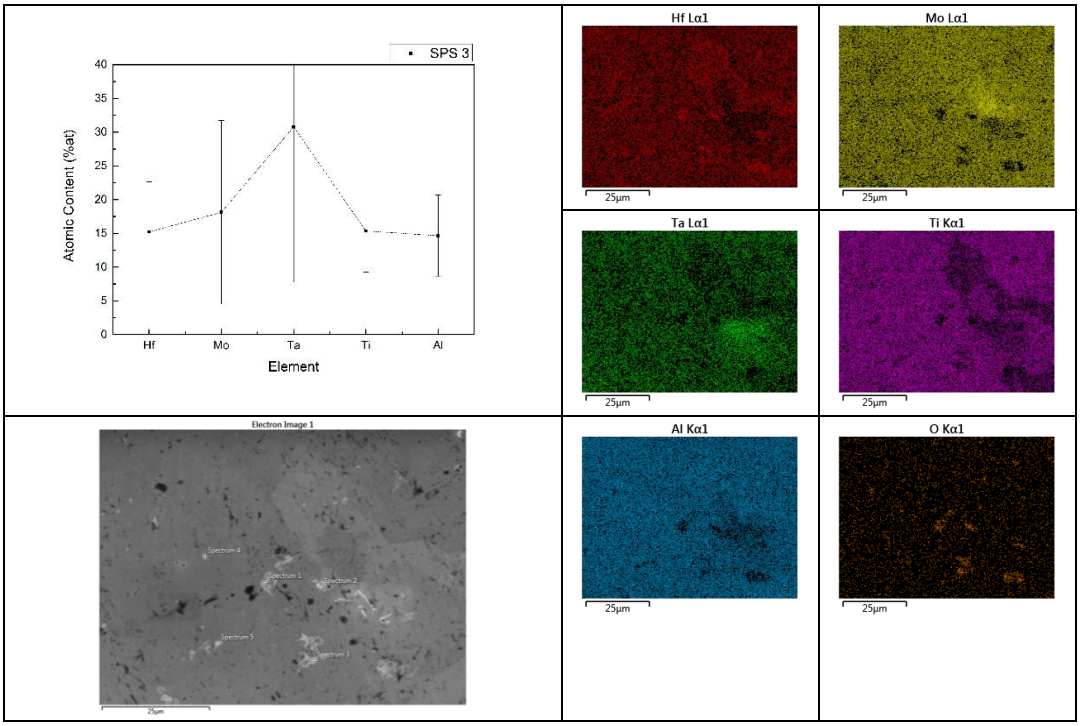

Figure 24: SEM and EDS results for SPS 3: Elements distribution(a), micrography(b) and mapping of sample(c).

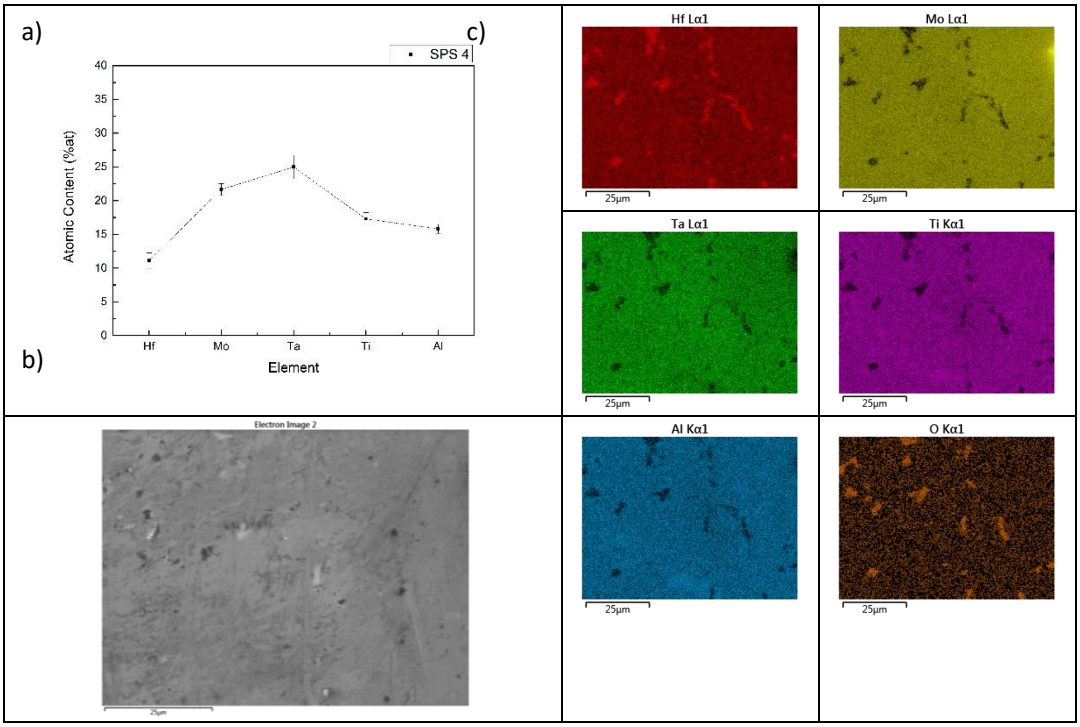

Figure 25

:SEM and EDS results for SPS 4: Elements distribution(a), micrography(b) and mapping of sample(c).

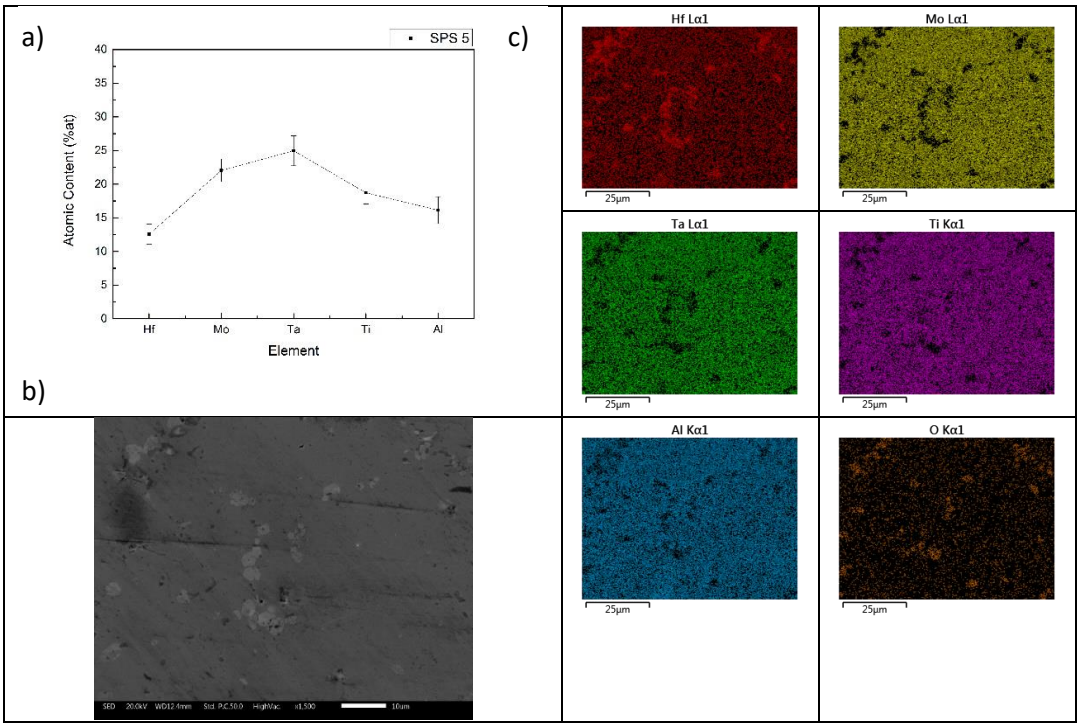

Figure 26: :SEM and EDS results for SPS 5: Elements distribution(a), micrography(b) and mapping of sample(c).

6.3. Density

In Table 13 it can be seen the results of the different HfMoTaTiAl samples and the HfMoTaTi system. With the introduction the aluminum in the system, a reduction of its density was achieved. However, this decrease was not as significant as it was expected according to the theoretical density calculated by the rule of mixture. This can be understood because if it is taken into account the results of the spectroscopies shown in SEM and EDS the atomic proportion of the aluminum is lower than what the theoretical one, making the reduction density of the samples lower than expected. The fact that the aluminum was lower than the theoretical one can be explained because the melting temperature of the aluminum is lower than the rest of the elements in the system. This makes that aluminum melts during the PCP process and part of it goes to the bottom of the sample during the sinter process. After the sinter the samples are grinded and polished. During this steps part of the material closer to the surface, which is where aluminum will have a higher content, is erased, reducing the amount of aluminum.

Table 13: Density results of the different samples of the HfMoTaTiAl system and HfMoTaTi

Sample	Density (g/cm^3)
SPS 1	9.8±0.1
SPS 2	10.0±0.1
SPS 3	10.0±0.1
SPS 4	10.5±0.1
SPS 5	9.9±0.1
HfMoTaTi	11.9±0.1

6.4. Hardness

As expected from the results of the literature[1], [7], [12], the introduction of aluminum in the system has considerably increased its hardness compared to its parent alloy as it can be seen in Figure 27. The hardness in HfMoTaTiAl system was 660 ± 30Hv while in the system without aluminum, HfMoTaTiAl, was 600 ± 10Hv. This means that the introduction of aluminum has increased between a 6% and 15% compared to the system without aluminum which is a substantial amount. It can also be noticed that the hardness of the HfMoTaTiAl system is higher than others with a similar composition like the ones showed in Figure 13, obtained from [12]. In this case not only the aluminum has to be taken into account that the processing method in these alloys was via arc-melting, and therefore via a liquid-state process, giving an as-cast microstructure. The indentation of sample SPS4 is shown in Figure 28. No crack was formed around the indentation, implying good fracture toughness of the sample.

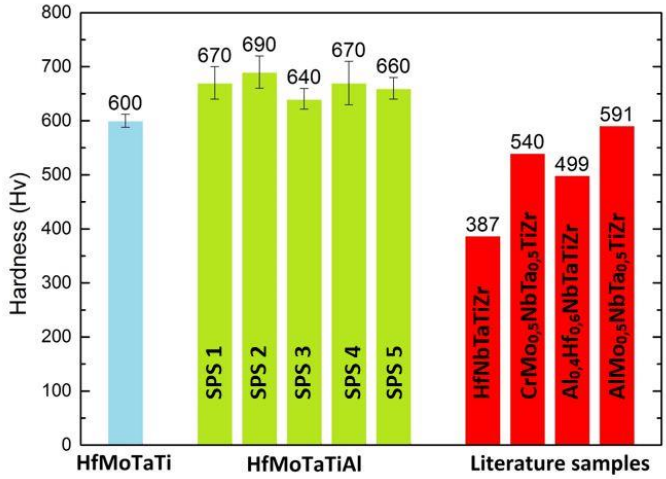

Figure 27: hardness results of the system HfMoTaTi (blue column) and the fabricated HfMoTaTiAl samples (green columns). Red columns represent the hardness of similar systems with/without aluminum obtained from [12]**.**

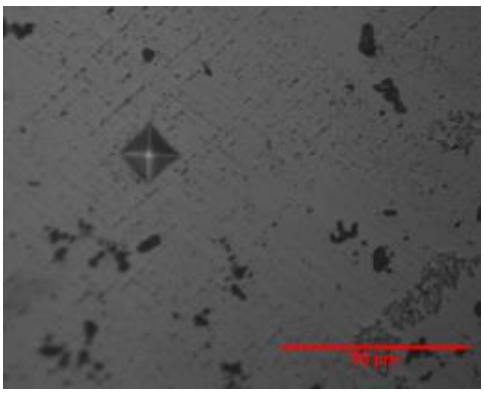

Figure 28: Deformation of the sample SPS 4 after the hardness test

6.5. Oxidation resistance

In Figure 29 it can be seen that the sample weight increase by increasing the temperature. The oxidation process begins at around 600ºC in both tests.

In test 1 (Figure 29a) after four hours of experiment the speed of weight gain is reduced but it doesn't reach a stabilization of the weight after 24 hours. At first it was considered that the time of the test wasn't enough to reach a stabilization of the weight gain as in other oxidation tests made in different articles the stabilization of the weight is achieved around 40 to 50 hours of test [15]–[19].

Another important factor that has to be taken into account is that molybdenum oxide volatilizes at lower temperature than 1200°C and therefore the weight gain doesn't fully represent the oxidation of the sample as there is also a weight loss. This has been proven reaffirmed during the EDS test as no molybdenum was present in the surface of the oxide layer as it can be seen in Figure 30. In order to acknowledge the total amount of oxidized material it is required to analyze the exhausted gas during the test using a mass spectrometer. In Figure 31 it can be seen that the oxide layer surface seems to be porous, making it easier for the oxygen to reach the metal surface of the sample.

BET results showed a high surface area per gram: 2.089m^2/g in the sample used in test 1. This confirmed the SEM results as the oxide layer generated during the test is porous and therefore it doesn't protect the metallic substrate. One possible reason is that when molybdenum oxide was formed, it tended to travel to the sampler surface and consequently penetrated the oxide layer and made it more porous.

In the second test, the temperature of the test was reduced and the time increased. With this second test it was expected to reach stabilization of the weight gained ruing the process but after 50 hours, it showed a linear growth once the barrier of 600°C was surpassed and the oxidation process was initiated. This linear growth confirms that the oxide layer doesn't protect the metal from the oxygen in the atmosphere.

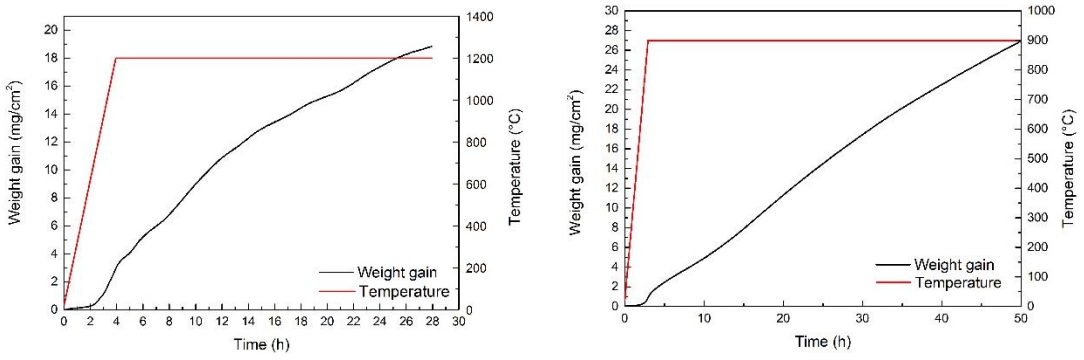

Figure 29: Weight gain and temperature curve during the oxidation resistance for test 1: 1200°C for 24h (a) and test 2: 900°C for 50h.

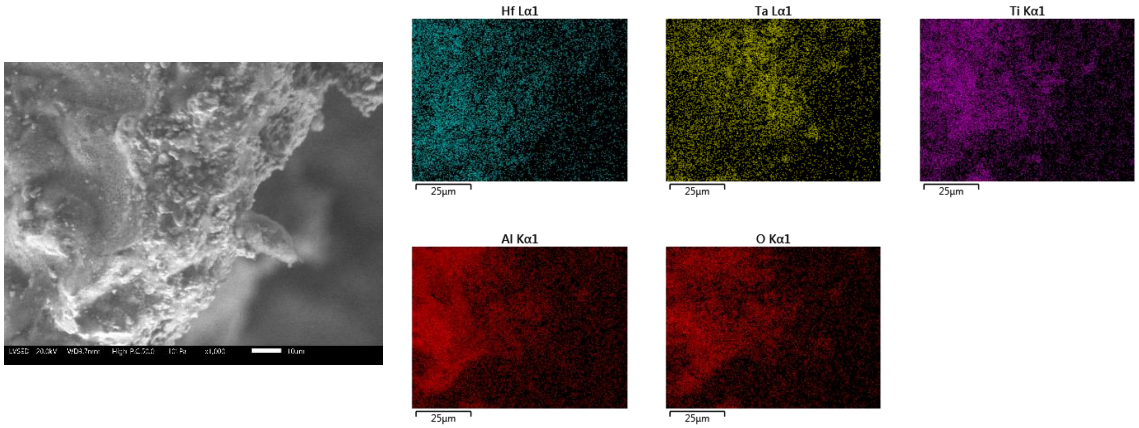

Figure 30: Micrography and EDS result of the oxide layer of the sample used in test 1: 1200°C for 24h.

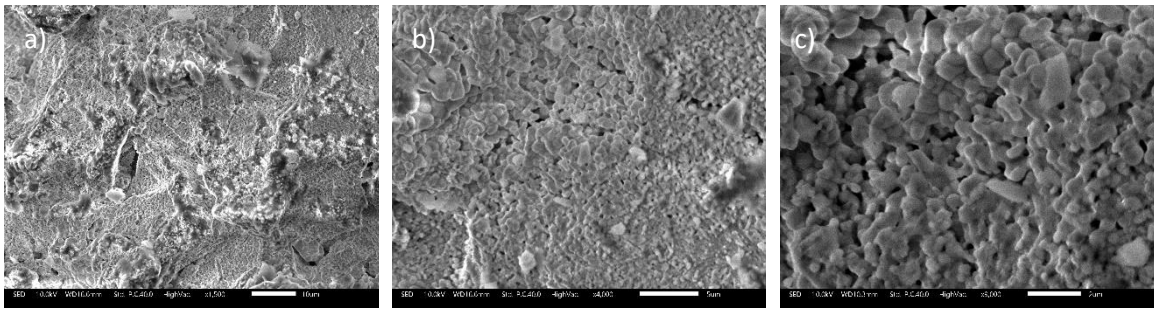

Figure 31: Micrographies of the oxide layer's surface of the sample used in test 1: 1200°C for 24h. (a) at 1500x, (b) 4000x and (c) 9000x.

7. CONCLUSIONS

In this project HfMoTaTiAl high entropy alloy was fabricated and investigated. With XRD and it was proved that the system was organized in a BCC structure. The most optimized temperature curves for the PCP solid state process have been determined to be SPS4 and SPS5 as their samples are the ones with the most homogeneous distribution of elements in the lattice. This is due to molybdenum and tantalum require a high activation energy for diffusion.

As expected, the addition of aluminum in the system improved the system properties: density was reduced by 17% while hardness increased between 6% and 15%.

The oxidation resistance of the alloy is not exceptional. According to the BET results, the oxide layer generated during the test is porous. One explanation of the bad performance of the oxide layer to be passivated may be that molybdenum oxide volatizes and therefore it pierces the oxide layer, leaving unprotected the metal surface of the sample.

In order to fully characterize the HfMoTaTiAl system there are still different tests to be done. A future work proposal is proposed in the next section.

8. FUTURE WORK

In order to extent the research of this project, some guidelines for the future work are recommended.

8.1. Sample preparation

HfO_2 was found in the hafnium raw material that was used to sinter the samples. Therefore another batch is required to be sintered in order to analyze its macroscopic properties such as mechanical properties in a compression test.

Another important point taken into account is the grain size of the raw materials. In order to make sure that the elements with high activation energy (molybdenum and tantalum) are distributed in the crystal structure as homogeneous as possible, it is recommended to use smaller grain sizes to improve the diffusion process.

In order to make sure that there are no impurities in the raw materials, check the particle size of the powders used and that there are no agglomerates it is recommended to use SEM and EDS in the raw materials and the mixture of the powders after the milling. If there are agglomerates use ultrasounds to sonicate the powders should disaggregate them.

8.2. Characterization of HfMoTaTiAl

As it has been said in the previous section the mechanical properties in a macroscopic scale haven't been characterized yet. As this material is expected to be used in high temperature conditions the tests proposed to do in the next batches of this alloy are focused in this requirement.

8.2.1. Compression tests

In order to understand the mechanical properties of the HfMoTaTiAl system it is required to do a mechanical test. From all the different possible tests the compression test is the one that requires the most simple geometry taken into account the synthesis process is pulse current processing. Other methods like a tensile test would require a bigger samples (therefore more material used per sample of already quite expensive raw materials) more probabilities to have a least homogeneous structure and a posterior machining of the samples. As the high temperature behavior is important to take into account the tests should be done at different temperatures so it can be seen how it influences its mechanical properties. A proposed scale of temperatures would be room temperature, 600°C, 800°C, 1000°C and 1200°C. These temperatures have been chosen as these temperatures have been chosen in similar alloy systems by Senkov et al [12] and it may be a good idea to use the same conditions in order to compare the results.

8.2.2. Creep tests

As these materials are expected to be subjected to high temperatures, creep of the material should be taken into account. Creep is usually studied in these alloys using microidentation equipment with a spherical tip [20]–[22]. The samples prepared by Ma et al. [21], [22] are films prepared via magneton sputtering with a thickness of 1.45 μm for these tests in the literature were made via magnetron sputtering. In the case of Lee [20] samples were prepared by arc-melting and had a disk shape with a radius of 5mm and a thickness of 0.83mm. Using a geometry similar to [20] should be achievable using PCP technique.

8.3. Improvement of the material for high temperature applications

As in all materials, not only the bulk material is important to understand its performance but it is also crucial to pay attention to other factors such as secondary phases and interfaces. In high

temperature applications creep is an important factor and it has two different ways to act: according to the viscous law, when the temperature is low enough to hinder the movement of dislocations, and the potential law, when dislocations can move freely through the bulk of the crystal.

In the first case (viscous law) the creep resistance is increased reducing the amount of grain boundaries. This situation is not possible to be achieved via PCP as the sinter process starts from different grains. In the second case (potential law) the creep resistance is achieved by blocking the path of dislocations through the bulk of the material. The common way to achieve it is using stable precipitates at high temperature. Usually these precipitates are silicon nitride, silicon carbide or oxides. As creep acts under the potential law, this technique may be feasible to improve the high temperature creep resistance for the HfMoTaTiAl system.

9. BIBLIOGRAPHY

[1] M. C. Gao, P. K. Liaw, J.-W. Yeh, and Y. Zhang, *High-entropy alloys: Fundamentals and applications*. 2016.

[2] M.-H. Tsai and J.-W. Yeh, "High-Entropy Alloys: A Critical Review," *Mater. Res. Lett.*, vol. 2, no. 3, pp. 107–123, 2014.

[3] D. B. Miracle and O. N. Senkov, "A critical review of high entropy alloys and related concepts," *Acta Mater.*, vol. 122, pp. 448–511, 2017.

[4] J. W. Yeh, "Recent progress in high-entropy alloys," *Ann. Chim. Sci. des Mater.*, vol. 31, no. 6, pp. 633–648, 2006.

[5] A. Takeuchi and A. Inoue, "Calculations of mixing H and mismatch S for ternary amorphous alloys.pdf." Materials transactions, JIM, Sendai, p. 1372 to 1378, 2000.

[6] B. S. Murty, J. W. Yeh, and S. Ranganathan, "High Entropy Alloys," *High Entropy Alloy.*, no. January, pp. 159–169, 2014.

[7] C.-J. Tong *et al.*, "Mechanical Performance of the AlxCoCrCuFeNi High-Entropy Alloy System with Multiprincipal Elements," *Metall. Mater. Trans. A*, vol. 36, no. 4, pp. 881–893, 2005.

[8] C. C. Juan *et al.*, "Solution strengthening of ductile refractory HfMoxNbTaTiZr high-entropy alloys," *Mater. Lett.*, vol. 175, pp. 284–287, 2016.

[9] C. M. Lin, C. C. Juan, C. H. Chang, C. W. Tsai, and J. W. Yeh, "Effect of Al addition on mechanical properties and microstructure of refractory AlxHfNbTaTiZr alloys," *J. Alloys Compd.*, vol. 624, pp. 100–107, 2015.

[10] O. N. Senkov, J. M. Scott, S. V. Senkova, D. B. Miracle, and C. F. Woodward, "Microstructure and room temperature properties of a high-entropy TaNbHfZrTi alloy," *J. Alloys Compd.*, vol. 509, no. 20, pp. 6043–6048, 2011.

[11] O. N. Senkov, G. B. Wilks, D. B. Miracle, C. P. Chuang, and P. K. Liaw, "Refractory high-entropy alloys," *Intermetallics*, vol. 18, no. 9, pp. 1758–1765, 2010.

[12] O. N. Senkov, S. V. Senkova, and C. Woodward, "Effect of aluminum on the microstructure and properties of two refractory high-entropy alloys," *Acta Mater.*, vol. 68, pp. 214–228, 2014.

[13] A. Takeuchi and A. Inoue, "Classification of Bulk Metallic Glasses by Atomic Size Difference, Heat of Mixing and Period of Constituent Elements and Its Application to Characterization of the Main Alloying Element," *Mater. Trans.*, vol. 46, no. 12, pp. 2817–2829, 2005.

[14] N. L. Peterson, "Diffusion in Refractory Metals," vol. 18, no. 4, pp. 203–210, 1960.

[15] B. Gorr, M. Azim, H. J. Christ, T. Mueller, D. Schliephake, and M. Heilmaier, "Phase equilibria, microstructure, and high temperature oxidation resistance of novel refractory high-entropy alloys," *J. Alloys Compd.*, vol. 624, pp. 270–278, 2015.

[16] B. Gorr *et al.*, "High temperature oxidation behavior of an equimolar refractory metal-based alloy [Formula presented] with and without Si addition," *J. Alloys Compd.*, vol. 688, pp. 468–477, 2016.

[17] C. M. Liu, H. M. Wang, S. Q. Zhang, H. B. Tang, and A. L. Zhang, “Microstructure and oxidation behavior of new refractory high entropy alloys,” *J. Alloys Compd.*, vol. 583, pp. 162–169, 2014.

[18] A. Raphel, S. Kumaran, K. V. Kumar, and L. Varghese, “Oxidation and Corrosion resistance of AlCoCrFeTiHigh Entropy Alloy,” *Mater. Today Proc.*, vol. 4, no. 2, pp. 195–202, 2017.

[19] T. M. Butler and M. L. Weaver, “Oxidation behavior of arc melted AlCoCrFeNi multi-component high-entropy alloys,” *J. Alloys Compd.*, vol. 674, pp. 229–244, 2016.

[20] D. H. Lee *et al.*, “Spherical nanoindentation creep behavior of nanocrystalline and coarse-grained CoCrFeMnNi high-entropy alloys,” *Acta Mater.*, vol. 109, pp. 314–322, 2016.

[21] Y. Ma, G. J. Peng, D. H. Wen, and T. H. Zhang, “Nanoindentation creep behavior in a CoCrFeCuNi high-entropy alloy film with two different structure states,” *Mater. Sci. Eng. A*, vol. 621, pp. 111–117, 2015.

[22] Y. Ma, Y. H. Feng, T. T. Debela, G. J. Peng, and T. H. Zhang, “Nanoindentation study on the creep characteristics of high-entropy alloy films: fcc versus bcc structures,” *Int. J. Refract. Met. Hard Mater.*, vol. 54, pp. 395–400, 2016.